The Geometric Structure of the Brain Fiber Pathways

Van J. Wedeen *et al.*

Science **335**, 1628 (2012);
DOI: 10.1126/science.1215280

Science (print ISSN 0036-8075; online ISSN 1095-9203) is published weekly, except the last week in December, by the American Association for the Advancement of Science, 1200 New York Avenue NW, Washington, DC 20005.

(fig. S13), and was strongest when the GoC population was sparsely activated by chemical excitatory synaptic inputs (fig. S14).

Our results show that the passive properties of GoC dendrites confer distance-dependent sublinear chemical synaptic integration. This weakens the impact of distal excitatory inputs. However, the high density of dendritic GJs in the molecular layer enables PF synaptic charge to flow into the dendrites of neighboring GoCs. This GJ-mediated lateral excitation counteracts the effects of sublinear dendritic behavior by enabling distal inputs to drive network activity more effectively. Dendritic GJs therefore counteract the problem of dendritic saturation (*24*) without the need to boost electrically remote synaptic input with active dendritic conductances (*25*). A key role of interneurons is to counteract and balance network excitation. The combination of passive dendrites and dendritic GJs facilitates this by enabling a larger fraction of interneurons to respond to localized patches of synaptic excitation. Our results reveal how GJs on inhibitory interneuron dendrites could contribute to spatial averaging, which has been proposed in the retina (*26*) and excitatory olfactory neurons in insects (*27*), and to the broad tuning of inhibitory interneurons in cortex (*28*). These mechanisms are also likely to contribute to gain control in the granule cell layer through PF-mediated feedback (*29*), and it seems likely that interneurons in cortical and subcortical structures (*7*) use similar mechanisms. Our results suggest that interneurons do not operate as fully independent neuronal units but share charge during chemical synaptic excitation and thus exhibit features of a syncitium.

References and Notes

1. T. F. Freund, G. Buzsáki, *Hippocampus* **6**, 347 (1996).
2. P. Jonas, J. Bischofberger, D. Fricker, R. Miles, *Trends Neurosci.* **27**, 30 (2004).
3. F. Pouille, M. Scanziani, *Science* **293**, 1159 (2001).
4. C. J. McBain, A. Fisahn, *Nat. Rev. Neurosci.* **2**, 11 (2001).
5. H. Hu, M. Martina, P. Jonas, *Science* **327**, 52 (2010).
6. M. Martina, I. Vida, P. Jonas, *Science* **287**, 295 (2000).
7. B. W. Connors, M. A. Long, *Annu. Rev. Neurosci.* **27**, 393 (2004).
8. R. T. Kanichay, R. A. Silver, *J. Neurosci.* **28**, 8955 (2008).
9. S. Dieudonne, *J. Physiol.* **510**, 845 (1998).
10. K. Vervaeke *et al.*, *Neuron* **67**, 435 (2010).
11. G. P. Dugué *et al.*, *Neuron* **61**, 126 (2009).
12. A. Losonczy, J. C. Magee, *Neuron* **50**, 291 (2006).
13. T. Nevian, M. E. Larkum, A. Polsky, J. Schiller, *Nat. Neurosci.* **10**, 206 (2007).
14. L. Forti, E. Cesana, J. Mapelli, E. D'Angelo, *J. Physiol.* **574**, 711 (2006).
15. J. C. Magee, E. P. Cook, *Nat. Neurosci.* **3**, 895 (2000).
16. S. R. Williams, G. J. Stuart, *Science* **295**, 1907 (2002).
17. H. Ohishi *et al.*, *Neuron* **13**, 55 (1994).
18. B. P. Vos, A. Volny-Luraghi, E. De Schutter, *Eur. J. Neurosci.* **11**, 2621 (1999).
19. P. L. van Kan, A. R. Gibson, J. C. Houk, *J. Neurophysiol.* **69**, 74 (1993).
20. S. Solinas *et al.*, *Front. Cell Neurosci.* **1**, 2 (2007).
21. S. J. Cruikshank *et al.*, *Proc. Natl. Acad. Sci. U.S.A.* **101**, 12364 (2004).
22. M. R. Deans, J. R. Gibson, C. Sellitto, B. W. Connors, D. L. Paul, *Neuron* **31**, 477 (2001).
23. P. Gleeson, V. Steuber, R. A. Silver, *Neuron* **54**, 219 (2007).
24. W. Rall, *J. Neurophysiol.* **30**, 1138 (1967).
25. S. Cash, R. Yuste, *Neuron* **22**, 383 (1999).
26. S. A. Bloomfield, B. Völgyi, *Nat. Rev. Neurosci.* **10**, 495 (2009).
27. E. Yaksi, R. I. Wilson, *Neuron* **67**, 1034 (2010).
28. A. M. Kerlin, M. L. Andermann, V. K. Berezovskii, R. C. Reid, *Neuron* **67**, 858 (2010).
29. D. Marr, *J. Physiol.* **202**, 437 (1969).

Acknowledgments: Funded by U.K. Biotechnology and Biological Sciences Research Council (BBSRC) (F005490), Medical Research Council (G0400598), and Wellcome Trust (064413). R.A.S. holds a Wellcome Trust Principal Research Fellowship (095667) and a European Research Council (ERC) Advanced Grant, Z.N. a Wellcome Trust Project Grant and an ERC Advanced Grant, and A.L. a Janos Bolyai Scholarship. We thank D. Paul for the $Cx36^{-/-}$ mice; E. Chaigneau, T. Branco, and P. Gleeson for help; D. Attwell, M. Farrant, H. Hu, D. Kullmann, J. Rothman, and D. Ward for comments on the manuscript; and T. Fernandez-Alfonso, H. Hu, and D. Ruedt for discussions.

Supporting Online Material

www.sciencemag.org/cgi/content/full/science.1215101/DC1
Materials and Methods
Figs. S1 to S15
References (*30*–*45*)

11 October 2011; accepted 21 February 2012
Published online 8 March 2012;
10.1126/science.1215101

The Geometric Structure of the Brain Fiber Pathways

Van J. Wedeen,[1]* Douglas L. Rosene,[2] Ruopeng Wang,[1] Guangping Dai,[1] Farzad Mortazavi,[2] Patric Hagmann,[3] Jon H. Kaas,[4] Wen-Yih I. Tseng[5]

The structure of the brain as a product of morphogenesis is difficult to reconcile with the observed complexity of cerebral connectivity. We therefore analyzed relationships of adjacency and crossing between cerebral fiber pathways in four nonhuman primate species and in humans by using diffusion magnetic resonance imaging. The cerebral fiber pathways formed a rectilinear three-dimensional grid continuous with the three principal axes of development. Cortico-cortical pathways formed parallel sheets of interwoven paths in the longitudinal and medio-lateral axes, in which major pathways were local condensations. Cross-species homology was strong and showed emergence of complex gyral connectivity by continuous elaboration of this grid structure. This architecture naturally supports functional spatio-temporal coherence, developmental path-finding, and incremental rewiring with correlated adaptation of structure and function in cerebral plasticity and evolution.

The organizing principles of cerebral connectivity remain unclear. In the brainstem and spinal cord, fiber pathways are organized as parallel families derived from the three principal axes of embryonic development: the rostro-caudal, the medio-lateral (or proximo-distal), and the dorso-ventral (*1*–*6*). In the forebrain of advanced species, however, corresponding patterns of connectivity have yet to be established. Many studies of evolution, development, and gene expression point to a geometric organization of cerebral fiber pathways similar to that of the brainstem (*3*–*5*, *7*–*9*), and functional studies (*10*–*13*) also suggest that connectivity is geometrically organized. Several leading theories of cerebral function (*14*–*17*) propose geometric organization at multiple scales. However, high-resolution studies of cerebral connectivity with tract tracers have given only limited evidence of geometric organization (*10*–*12*, *18*, *19*).

A challenge in the investigation of cerebral structure and connectivity can be traced to the common occurrence of distinct pathways within the same small volumes of tissue, or "path crossing." Crossing is a pervasive feature of brain structure and may be essential for efficient connectivity (*20*, *21*). Owing to crossing, the mapping of connectivity must untangle pathways from cellular to macroscopic scales simultaneously (*22*, *23*). This was accomplished with tract tracers methods, which are considered a gold standard (*18*, *19*). Tracer studies inject compounds into the live brain and allow them to disperse by means of axonal transport, marking individual axons over large distances. However, these can map only a small fraction of the pathways in any single brain and are not feasible in humans. Thus, the discovery and analysis of the structural relationships between pathways—and their context within cerebral connectivity—has remained challenging (*18*, *19*, *24*).

To address these limitations, methods have been developed to map the fiber pathways of the

[1]Department of Radiology, Massachusetts General Hospital (MGH), Harvard Medical School and the MGH/Massachussetts Institute of Technology Athinoula A. Martinos Center for Biomedical Imaging, Building 129, 13th Street, 2nd Floor, Charlestown, MA 02129, USA. [2]Department of Anatomy and Neurobiology, Boston University, Medical Campus, 700 Albany Street, W701, Boston, MA 02118, USA. [3]Department of Radiology, University Hospital Center–University of Lausanne, Rue du Bugnon, 46, CH-1011 Lausanne, Switzerland. [4]Department of Psychology, College of Arts and Sciences, Vanderbilt University, 301 Wilson Hall, 111 21st Avenue South, Nashville, TN 37240, USA. [5]Department of Radiology, Center for Optoelectronic Biomedicine, National Taiwan University College of Medicine, 1 Jen-Ai Rd, Taipei, Sec 1, 100 Taiwan.

*To whom correspondence should be addressed. E-mail: van@nmr.mgh.harvard.edu

brain through use of diffusion magnetic resonance imaging (MRI). Diffusion MRI creates multidimensional contrast that is representative of the distribution of fiber orientations at each location in the tissue (*21*). Though of lower resolution than tract tracing, diffusion MRI is noninvasive, applicable to humans and synoptic, and able to map the connectional anatomy of a single brain in its entirety, including spatial correlations between pathways. These correlations represent the mesoscale structure of connectivity, within the scope of which are the questions of whether cerebral pathways are discrete versus continuous and the detailed character of the spatial organization of connectivity.

To probe the spatial relations between the pathways of the brain, we analyzed path-adjacency and path-crossing in four nonhuman primate species and in humans. Diffusion spectrum MRI (DSI) was acquired in whole-brain specimens ex vivo in rhesus, owl monkey, marmoset, and the prosimian galago, and in vivo in subjects (515 directions; pathways were computed with deterministic streamline integration) (*21*). To demonstrate pathways' structural relationships, we augmented interactive software to compute for any path the set of all paths with which it shares one or more voxels, termed its path neighborhood.

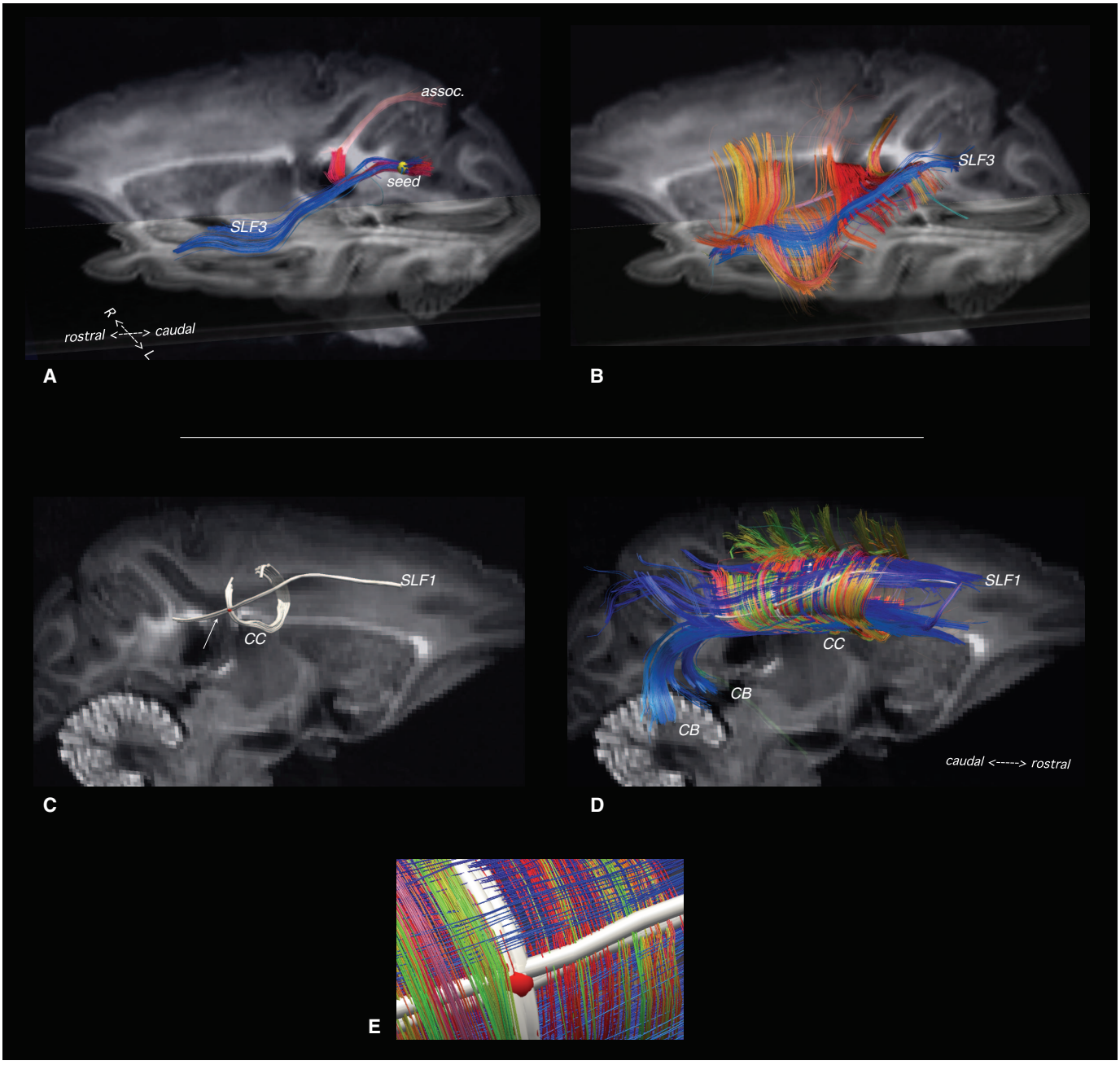

Fig. 1. Neighborhood structure of cerebral pathways. (**A**) MRI analog of tracer injection. A major association pathway of the rhesus forebrain SLF3 (blue) was identified by its termination in a selected region (yellow sphere in the parietal lobule). A co-terminus association pathway (red) is noted. These pathways appear as isolated structures. (**B**) The path neighborhood of SLF3 is identified: a curved sheet of parallel paths (orange) that cross SLF3 nearly orthogonally. (**C** to **E**) A path neighborhood in the rhesus frontal lobe (right lateral view). (C) A region (red sphere, arrow) is selected in the white matter deep to the cingulate gyrus. The paths incident on this region (white) are near-orthogonal paths within the corpus callosum and SLF1. (D) The set of all paths incident on these paths in (C) forms a curved sheet of interwoven orthogonal pathways [(E) shows detail], including mutually parallel transverse paths of the callosum (red to green) and longitudinal paths (blue) within SLF1 and the cingulum bundle (CB). No other path orientations were evident.

The character of a typical cerebral path neighborhood is illustrated in Fig. 1. In Fig. 1A, an association pathway—rhesus monkey superior longitudinal fasciculus-3 (SLF3)—is identified by its termination within the parietal lobe; this is the MRI analog of a tracer injection (*25*). So defined, this pathway appeared as an almost isolated structure. In Fig. 1B, the path neighborhood of SLF3 was identified and was astonishingly simple. It entirely consists of a single curved two-dimensional (2D) sheet of paths, all mutually parallel, transversely oriented, and all crossing SLF3 at nearly right angles.

To investigate neighborhood structure independent of path identifications, we adopted the following procedure: select a small region, identify its incident paths, and compute the paths incident on these paths, their neighborhood. This was performed in the rhesus frontal lobe, as illustrated in Fig. 1, C to E. The path neighborhood comprises two sets—transverse callosal paths and longitudinal paths of the cingulum and SLF1—that crossed like the warp and weft of a fabric as a near-orthogonal grid. Thus, these paths formed a single biaxial system. This pattern was typical of cerebral white matter.

The 3D structure of cerebral pathways was demonstrated through analysis of several path

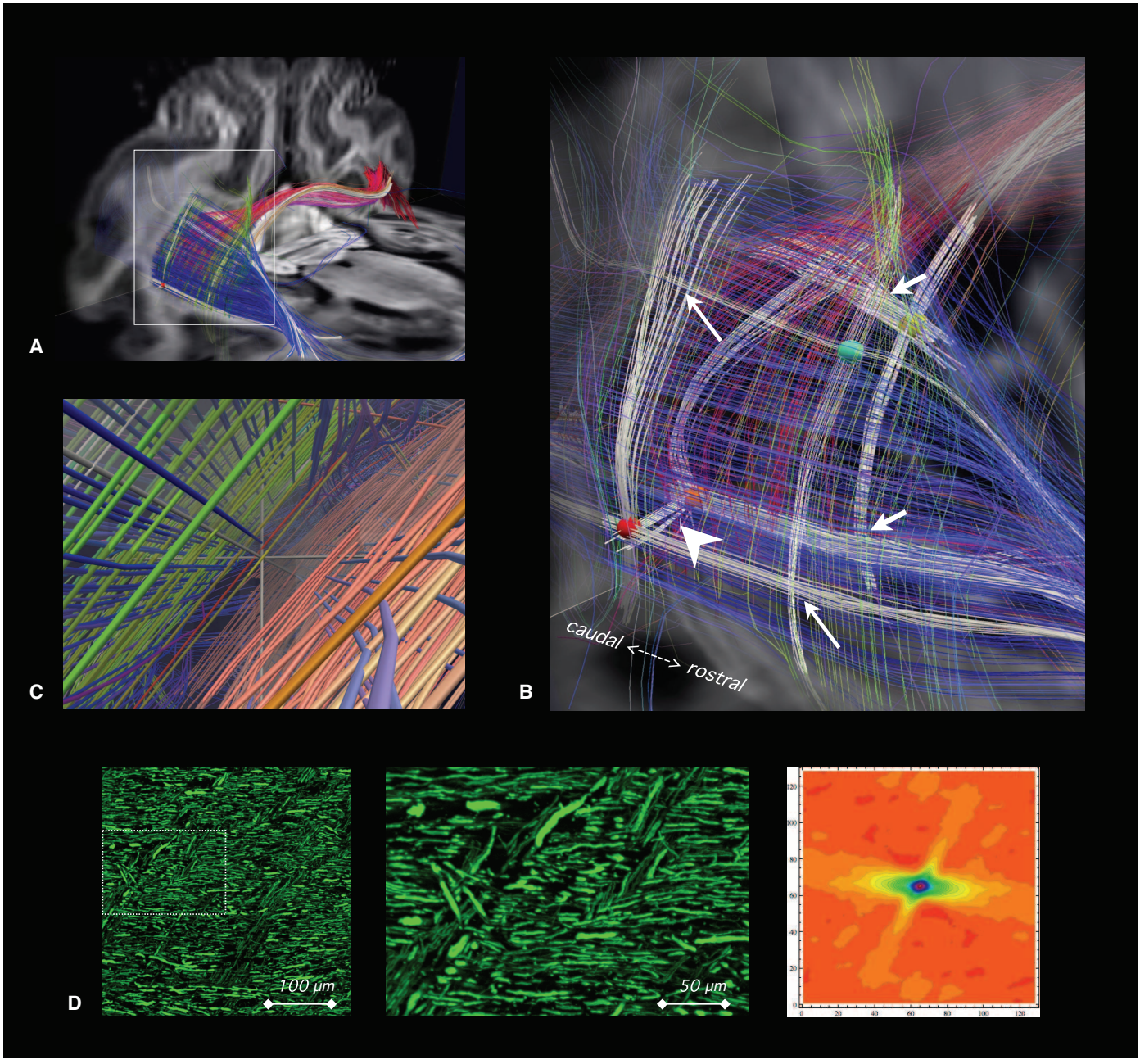

Fig. 2. Grid structure of cerebral pathways. The grid structure of the pathways of the sagittal stratum in the rhesus occipital lobe was demonstrated by means of neighborhood analysis. (**A** and **B**) Four seed regions were selected (spheres are indicated as superficial by red and green and as deep by yellow and orange), their paths identified (white), and neighborhoods computed (fronto-occipital fasciculus, blue; callosal paths, red and orange). The interior view along the axis of the structure (**C**) illustrates its character as an orthogonal grid. These neighborhoods comprised 2D sheets of closed quadrilaterals at each depth [(B), arrows]. The paths within each sheet were orthogonal: of the longitudinal fronto-occipital fasciculus (FOF) (blue) or the transverse callsum (red) and association system (green). Paths of the third mutually orthogonal direction (arrowhead), perpendicular to the local cortical surface, were noted. (**D**) Confocal microscopy of a sagittal slice oblique cut parallel to the lateral face of the sagittal stratum showed in-plane crossing of FOF (horizontal) and callosal paths (vertical oblique), and the 2D autocorrelation map of this microscopy, representative of the fiber orientations.

neighborhoods in a single region. Deep white matter of the occipital lobe—the sagittal stratum—of the rhesus monkey is shown in Fig. 2. Here, four seed regions were selected whose incident paths and their neighborhoods formed the edges and faces of a curved rectangular box, demonstrating that parallel grid structure of pathways was not limited to particular 2D surfaces but extended throughout entire 3D volumes. Paths in the third nearly orthogonal axis were also seen and no diagonal paths observed. Similar 3D organization was demonstrated in the highly curved midline system [supporting online material (SOM) text and fig. S1].

In all present studies, cerebral path crossings formed well-defined 2D sheets. For example, in Fig. 2B paths crossed (arrows) so as to form closed quadrilaterals that are elements of well-defined

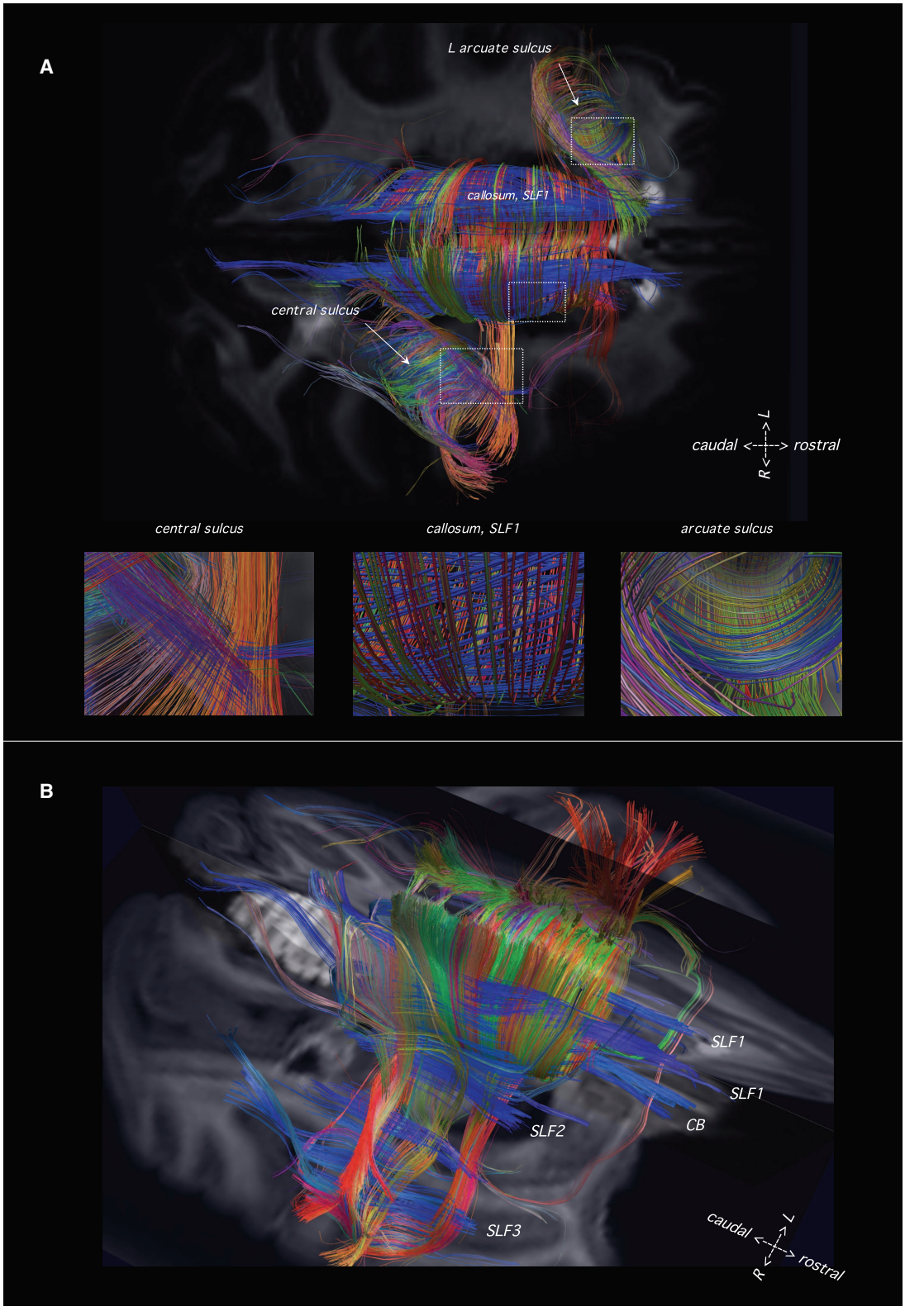

Fig. 3. Continuous grid structure of rhesus frontal lobes. (**A**) The grid structure of subcortical pathways was continuous within and between path neighborhoods. Three neighborhoods were constructed of the left arcuate and right central sulci and the midline. (Insets) All cortico-cortical pathways were highly curved elements in a sheet of interwoven paths in two nearly perpendicular orientations. The grid structure was continuous within and between neighborhoods. Path orientation was aligned with gyral topography in the acuate sulcus and but oblique in central sulcus, with spiral trajectories (violet). (**B**) Major pathways in deep white matter in the rhesus frontal lobe (from top left), including SLF 1-3, and the cingulum bundle (CB) (blue) were components of a single path-grid. Their intersecting pathways (green, orange, and red) are transverse, parallel at all scales, and cross orthogonally.

2D surfaces. Geometrically, this configuration is highly exceptional (*26*, *27*). Just as it is exceedingly unlikely that several points fall on a straight line, it is similarly improbable that two families of curves in 3D have any 2D surfaces in common. This sheet structure was found throughout cerebral white matter and in all species, orientations, and curvatures. Moreover, no brain pathways were observed without sheet structure. Further, because the processes of diffusion encoding, reconstruction, and tractography are purely local, limited to single or to adjacent voxels, whereas the spatial correlations entailed in this pattern were long-range and nonlinear, this structure could not be attributed to technical artifacts related to the imaging of diffusion (SOM text and fig. S2). A histological counterpart of the crossing structure of fiber pathways was observed with confocal microscopy: a tissue section through the rhesus monkey sagittal stratum cut parallel to the sheets of Fig. 2, A to C, that showed axons interweaving and crossing in two axes, which was confirmed by the orientation distribution of their spatial autocorrelation (*28*).

Grid structure of cerebral pathways was pervasive, coherent, and continuous with the three principal axes of development. In each region in Fig. 3A, continuous grid structure is demonstrated across several regions in the frontal lobes in rhesus monkey, including left arcuate sulcus,

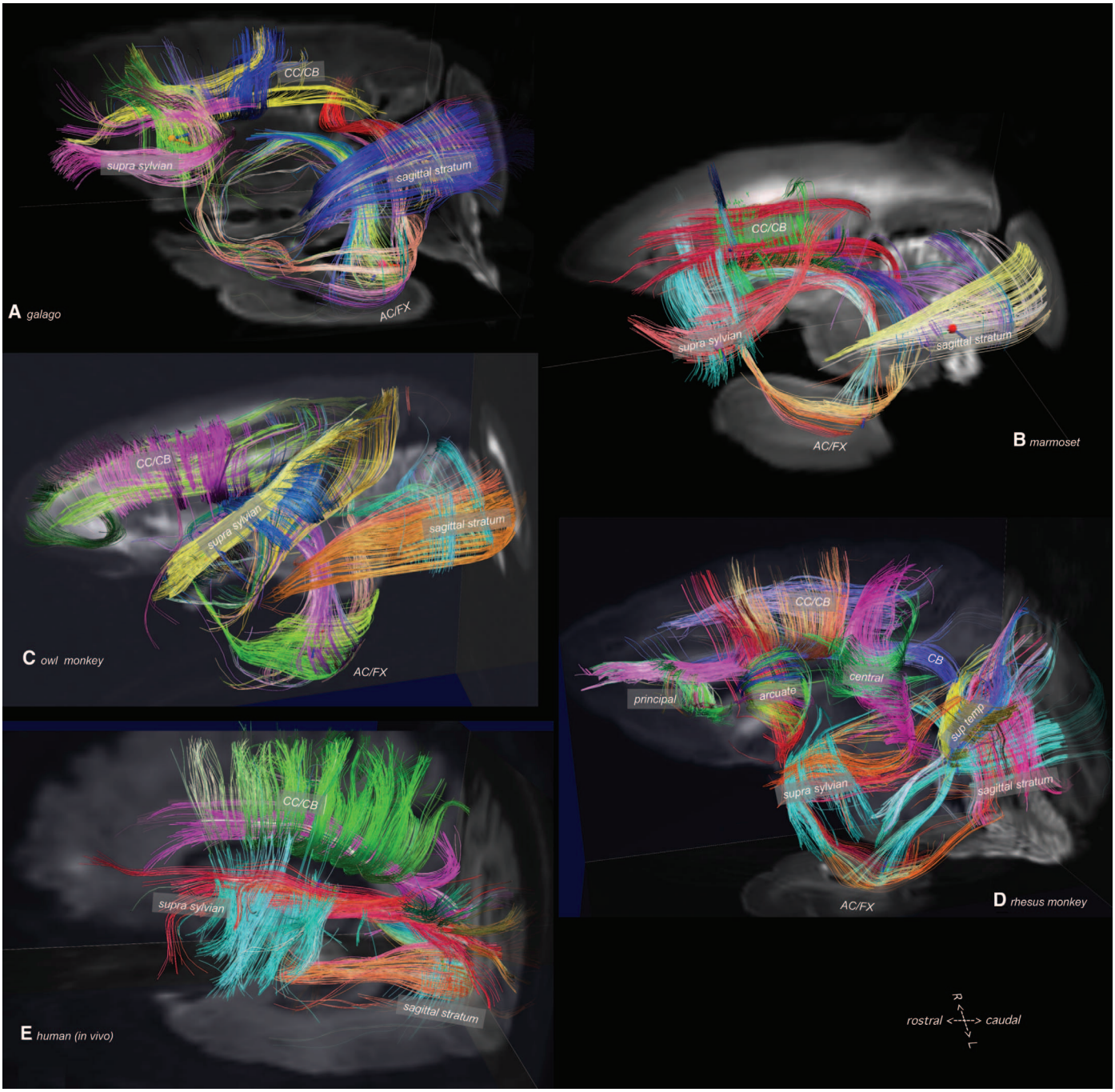

Fig. 4. Homologous cerebral grid structure in (**A**) galago, (**B**) marmoset, (**C**) owl monkey, (**D**) rhesus monkey, and (**E**) human, left lateral views. Homologous grid structures including those of the corpus callosum/cingulum bundle (CC/CB); sagittal stratum and supra-Sylvian region were identified in all species, and that of the anterior commissure and fornix (AC/FX) was resolved in all ex vivo studies [(A) to (D)]. In the rhesus monkey, grid structure is shown in gyri and sulci, including the principal, arcuate, and central sulci and the superior temporal gyrus, continuous as grids with those of the adjacent deep white matter.

midline callosal region, and right central sulcus. The grid orientations in central sulcus were not parallel to gyral topography but were oblique, following spiral trajectories. This contrasted with the temporal lobes, where path and gyral orientations were closely aligned (SOM text and fig. S3A).

In rhesus deep white matter, the major frontal association pathways were parallel elements of a single grid (Fig. 3B, SOM text, and fig. S4). These pathways were not highly distinct but continuous with their neighbors via sparse interposed parallel paths. This was consistent in analysis at multiple depths (SOM text and fig. S4). Thus, major longitudinal pathways of the frontal lobe as well as longitudinal U-fiber pathways could be considered local condensations of a single system that spans the frontal lobe. The grid structure of pathways of the cerebral mantle was continuous with those of the limbic system and basal ganglia (SOM text and fig. S3B).

To investigate how pathways may change course, we analyzed a known turn in a major cerebral pathway identified in the tracer studies of Schmahmann and Pandya in rhesus monkey (*17*). Tracer and DSI showed bifurcation of a frontal projection pathway into transverse and dorsoventral components. In lieu of diagonals, pathways were found to bifurcate and turn between axes (SOM text and fig. S5).

To investigate grid continuity in the cerebral hemisphere, widely separated path neighborhoods were constructed in owl monkey. Grid structure was maintained at all scales, from the single voxel, to the lobe, to the hemisphere (SOM text and fig. S6). Continuity of grid structure between superficial gyral and deep cerebral pathways was demonstrated through analysis of neighborhoods at sequential depths (SOM text and fig. S4). Grid structure in all three orthogonal axes was observed in the centrum semiovale, including the longitudinal and transverse paths and dorso-ventral projection paths. This was observed in the rhesus and in the human, in vivo and ex vivo (SOM text and fig. S7). Further validation of grid structure of cerebral pathways was obtained with an alternative MRI contrast mechanism of circular diffusion contrast (SOM text and fig. S8) (*29*), and the recognized triaxial structure of pathways of the brainstem was shown with present methods (SOM text and fig. S9).

Strong homology of deep cerebral grid structure was found across all species studied (Fig. 4). These included the grid systems of the callosum, sagittal stratum, and supra-Sylvian pathways, as well as the crossing of the fornix and anterior commissure in all species studied ex vivo at high resolution. In the rhesus monkey, central and subcortical grid structures (Fig. 4D), including those of the major frontal sulci (principal, arcuate, central), fit together continuously like a jigsaw puzzle (SOM text and figs. S3A, S4, and S6, owl monkey). Thus, we hypothesize that the complex connectivity of the cerebral mantle represents a continuous elaboration of the simpler core.

We have found that the fiber pathways of the forebrain are organized as a highly curved 3D grid derived from the principal axes of development. This structure has a natural interpretation. By the Frobenius theorem, any three families of curves in 3D mutually cross in sheets if and only if they represent the gradients of three corresponding scalar functions (*26*, *27*). Accordingly, we hypothesize that the pathways of the brain follow a base-plan established by the three chemotactic gradients of early embryogenesis (*30*). Thus, the pathways of the mature brain presents an image of these three primordial gradients, plastically deformed by development. This could be tested by obtaining diffusion MRI during cerebral embryogenesis and assessing the derivation of pathways from the primordial directions. Grid structure should restrict and simplify axonal path-finding compared with models that allow less constrained and less correlated connectivity within and between cerebral areas. If grid structure guides connectivity similar to the lane markers in a highway, then navigation would be reduced from a general 3D problem to a far simpler question of when to exit. In the brain, fibers growing in any axis would have a choice at each moment of just the four orthogonal directions perpendicular to their course. Grid structure would increase the efficacy of path orientation as a mechanism of axonal path-finding (*31*, *32*). Simultaneously, this structure supports incremental modification of connectivity by geometric modification within broad continuous families of parallel paths. Thus, the grid organization of cerebral pathways may represent a "default connectivity," on which adaptation of structure and function can both occur incrementally in evolution and development, plasticity, and function.

A grid organization of cerebral pathways has been suggested in several contexts. Katz *et al*. (*8*) hypothesized that a large-scale substrate of grid organization is applicable to forebrain development. Checkerboard organization of cortical Brodmann fields has been noted in visual areas of the temporal lobe (*1*) and frontal motor areas (*3*) in monkeys. In humans, Badre and D'Esposito (*13*) have suggested hierarchic organization of the frontal cortex along a rostro-caudal axis.

The correlation between grid and topographic orientations observed in the rhesus temporal lobe supports Van Essen's hypothesis relating cerebral folding to fiber tension (*33*); however, the variable relation of fiber structure and cortical folding observed in the frontal lobe merits further investigation. More recently, Clochoux *et al*. have derived from its patterns of folding a spherical coordinate system for the longitude and latitude of the human cerebral cortex (*34*). This coordinate system seems generally congruent with that implied by the present grid structure of pathways, and investigation of their relationship may shed light on the linkage in structure and development between cerebral gray matter and white matter.

Greater differentiation between pathways was observed in the more complex rhesus brain than in simpler species, suggesting that the evolutionary emergence of discrete pathways parallels the increasing cerebral complexity in the primate lineage. Functionally, pervasive cerebral organization with parallel paths and similar lengths would naturally support neural coding via spatial and temporal coherence (*16*).

The grid structure of cerebral pathways has implications for brain mapping: It suggests a simplifying framework and natural coordinate system (*35*) for the description of brain structure, its pathways, and connectivity; simplifies and constrains models of cerebral white matter; and indicates that topographic organization is characteristic of cerebral connectivity and not limited to a few major pathways. Of concern, present findings suggest that existing MRI tractography may underestimate sharp turning (*36*). It also provides a means to validate MRI tractography through consistency with grid structure.

References and Notes

1. W. His, *Die Abh. Kon. Sacuh. Ges. Wiss. Math. Phys. Kl.* **15**, 675 (1889).
2. S. Ramon y Cajal, *Histologie du Systeme Nerveux de l'Homme et des Vertebres* (A. Malone, Paris, 1909).
3. B. F. Kingsbury, *J. Comp. Neurol.* **32**, 113 (1920).
4. H. Bergquist, B. J. Kallen, *Comp. Neurol.* **100**, 627 (1954).
5. M. N. Bernside, A. G. Jacobsen, *Dev. Biol.* **18**, 537 (1968).
6. C. Nicholson, in *The Central Nervous System of Vertebrates*, R. Niewenhuys, H. J. ten Donkelaar, Eds. (Springer-Verlag, Berlin, 1998), vol. 1, chap 5.
7. R. Nieuwenhuys, *Brain Res. Bull.* **57**, 257 (2002).
8. M. J. Katz, R. J. Lasek, H. J. W. Nauta, *Neuroscience* **5**, 821 (1980).
9. L. Puelles, *Brain Behav. Evol.* **46**, 319 (1995).
10. E. A. DeYoe, D. J. Felleman, D. C. Van Essen, E. McClendon, *Nature* **371**, 151 (1994).
11. J. H. Kaas, *Anat. Rec. A Discov. Mol. Cell. Evol. Biol.* **281A**, 1148 (2004).
12. L. W. Swanson, *Brain Res. Brain Res. Rev.* **55**, 356 (2007).
13. D. Badre, M. D'Esposito, *Nat. Rev. Neurosci.* **10**, 659 (2009).
14. M. M. Mesulam, *Brain* **121**, 1013 (1998).
15. K. Friston, *Nat. Rev. Neurosci.* **11**, 127 (2010).
16. K. E. Stephan *et al*., *Philos. Trans. R. Soc. Lond. B Biol. Sci.* **356**, 1159 (2001).
17. J. D. Schmahmann, D. N. Pandya, *Fiber Pathways of the Brain* (Oxford Univ. Press, Oxford, 2006).
18. M. Abeles, *Corticonics* (Cambridge Univ. Press, Cambridge, 1991).
19. D. Mumford, *Biol. Cybern.* **66**, 241 (1992).
20. V. J. Wedeen, P. Hagmann, W. Y. Tseng, T. G. Reese, R. M. Weisskoff, *Magn. Reson. Med.* **54**, 1377 (2005).
21. V. J. Wedeen *et al*., *Neuroimage* **41**, 1267 (2008).
22. J. Klingler, *Schweiz. Arch. Neurol. Psychiatr.* **36**, 247 (1935).
23. W. J. S. Krieg, *Connections of the Cerebral Cortex* (Brain Books, Chicago, IL, 1963).
24. J. Livet *et al*., *Nature* **450**, 56 (2007).
25. J. D. Schmahmann *et al*., *Brain* **130**, 630 (2007).
26. W. P. Thurston, *Three Dimensional Tand Geometry*, S. Levy, Ed. (Princeton Univ. Press, Princeton, NJ, 1997) ch 3.7.
27. C. W. Meisner, K. S. Thorn, J. A. Wheeler, *Gravitation* (W. H. Freeman, San Francisco, 1973).
28. W.-Y. I. Tseng, V. J. Wedeen, T. G. Reese, R. N. Smith, E. F. Halpern, *J. Magn. Reson. Imaging* **17**, 31 (2003).
29. V. J. Wedeen, J. G. Dai, W.-Y. I. Tseng, R. Wang, T. Benner, *Proc. Intl. Soc. Mag. Reson. Med.* **14**, 851 (2006).
30. S. N. Sanson, F. J. Livesey, *Cold Spring Harb. Perspect. Biol.* **1**, a002519 (2009).
31. L. Vasung *et al*., *J. Anat.* **217**, 400 (2010).
32. A. Chédotal, L. J. Richards, *Cold Spring Harb. Perspect. Biol.* **2**, a001917 (2010).

33. D. C. Van Essen, *Nature* **385**, 313 (1997).
34. C. Clouchoux *et al.*, *Neuroimage* **50**, 552 (2010).
35. R. Nieuwenhuys, *Brain Struct. Funct.* **214**, 79 (2009).
36. P. J. Basser, S. Pajevic, C. Pierpaoli, J. Duda, A. Aldroubi, *Magn. Reson. Med.* **44**, 625 (2000).

Acknowledgments: The authors thank L. C. Abbate, J. W. Belliveau, D. A. Feinberg, B. R. Rosen, S. A. Wedeen, and M. W. Weiner for reviewing this manuscript; J. D. Schmahmann, B. I. Shraiman, R. Turner, H. E. Stanley, and T. J. Brady for their comments; K. Mansfield of the New England Primate Center and L. Worthylake of the Oregon National Primate Research Center for primate specimens; C. Devitt for myelin stains; and M. P. Frosch for human specimens. The content is solely the responsibility of the authors and does not necessarily represent the official views of the National Science Foundation, the National Institute Of Mental Health, or the National Institutes of Health. This work is directly supported by grants NSF PHY-0855161, NIH R01-MH652456, P41 RR-023953, P41 RR-14075, and The Human Connectome Project U01 MH093765. V.J.W. designed the methods of MRI acquisition, reconstruction, and analysis; acquired and analyzed the data; discovered the grid structure; and wrote the paper. W.-Y.I.T. collaborated in the development of theoretical, imaging, and anatomic ideas and methods. G.D. implemented MRI acquisition techniques, including hardware and pulse sequences; optimized protocols; and acquired ex vivo MRI. R.W. implemented analysis algorithms and created their user interface. J.H.K. and D.L.R. obtained and prepared specimens, participated in analyses, and contributed to this manuscript. F.M. optimized and obtained immunofluorescent microscopy. P.H. provided in vivo human studies. All authors discussed the results and commented on the manuscript. No author has a major competing interest to declare. All human studies were obtained after signed informed consent, with review and approval by the Institutional Review Board. Tissue specimens were studied as discarded materials, with review and approval by the Institutional Subcommittee on Animal Care. Human tissue specimens were studied as deidentified discarded materials, with review and approval by the Institutional Review Board.

Supporting Online Material
www.sciencemag.org/cgi/content/full/335/6076/1628/DC1
Materials and Methods
SOM Text
Figs. S1 to S9

13 October 2011; accepted 10 February 2012
10.1126/science.1215280

Hierarchical Genetic Organization of Human Cortical Surface Area

Chi-Hua Chen,[1] E. D. Gutierrez,[2] Wes Thompson,[1] Matthew S. Panizzon,[1] Terry L. Jernigan,[1,2] Lisa T. Eyler,[1,3] Christine Fennema-Notestine,[1,4] Amy J. Jak,[1,5] Michael C. Neale,[6] Carol E. Franz,[1,7] Michael J. Lyons,[8] Michael D. Grant,[8] Bruce Fischl,[9] Larry J. Seidman,[10] Ming T. Tsuang,[1,5,6] William S. Kremen,[1,5,6]*† Anders M. Dale[1,4,11]*

Surface area of the cerebral cortex is a highly heritable trait, yet little is known about genetic influences on regional cortical differentiation in humans. Using a data-driven, fuzzy clustering technique with magnetic resonance imaging data from 406 twins, we parceled cortical surface area into genetic subdivisions, creating a human brain atlas based solely on genetically informative data. Boundaries of the genetic divisions corresponded largely to meaningful structural and functional regions; however, the divisions represented previously undescribed phenotypes different from conventional (non–genetically based) parcellation systems. The genetic organization of cortical area was hierarchical, modular, and predominantly bilaterally symmetric across hemispheres. We also found that the results were consistent with human-specific regions being subdivisions of previously described, genetically based lobar regionalization patterns.

As early as the 1950s, Bergquist and Kallen postulated that the entire embryonic brain is divisible into an anteroposterior series of segmented neuromeres, each forming a complete ring around the brain's longitudinal axis (*1*). Almost 40 years later, experimental data showed that many gene expression domains respect segment boundaries in the embryonic vertebrate hindbrain, suggesting a role of genetic control in regional differentiation (*2*, *3*). This important finding prompted a search for similar genetic regulatory organization in other regions of the developing vertebrate brain (*4*). In particular, in the past decade the cerebral cortex has received substantial attention. Studies have shown, for example, that several signaling molecules and transcription factors are involved in establishing boundaries between mouse cortical regions (*5*, *6*). Animal data demonstrate that the regional or positional identity of cortical regions is defined by the combinatorial expression pattern of various genes controlling for regional differentiation, each of which is expressed in a graded and restricted pattern with distinct spatiotemporal characteristics (*7*). Little is known, however, about the genetic patterning underlying the human cortex. In our previous work (*8*), we showed that genetic patterning underlying the anteroposterior gradient and four basic cortical divisions of cortical surface area demonstrated in mouse models (*7*) also existed in the human cortex. Furthermore, region-specific cortical areal expansion in humans has been linked to specific genetic polymorphisms (*9*, *10*). We sought to go beyond the fundamental commonalities that humans share with other species and to investigate the genetic patterning specific to the human cortex with its 1000-fold increase in surface area relative to the mouse brain (*11*). In effect, we sought to develop a brain atlas of human cortical surface area that was based entirely on genetic correlations, rather than a priori structural or functional information.

To delineate the genetic patterning of the cortical area, we measured relative surface areal expansion using cortical surface reconstruction and spherical atlas mapping developed by Dale and colleagues (*12*–*14*). We divided the area measured at each location by the total surface area in order to account for global effects. Using the twin design, which compares monozygotic and dizygotic twins, we then estimated genetic correlations between different points on the cortical surface. These genetic correlations represent shared genetic influences on relative areal expansion between cortical regions (*15*). Details of these methods have been previously described (*8*, *16*). After computing pairwise genetic correlations, we used an unsupervised pattern recognition method—fuzzy cluster analysis (*17*)—to demarcate the genetic topography of cortical surface area based on the genetic correlations of relative surface area measures. To determine the appropriate number of clusters, we computed the widely used silhouette coefficient.

On the basis of the peak of the silhouette coefficients (fig. S1), we identified 12 natural clusters. These clusters correspond closely to meaningful structural and functional regions (Fig. 1), even though the registration procedure did not rely on prespecified anatomical landmarks; rather, it makes use of the continuous pattern of surface curvature (*13*). In describing the subdivisions, we use conventional labels, but these only approximate the observed clusters. Subdivisions of the frontal cortex include the motor-premotor, dorsolateral prefrontal cortex extending to the anterior and superior parts, dorsomedial frontal, and orbitofrontal (Fig. 1, clusters 1 to 4). Another cluster is found between the frontal and parietal cortices, extending from pars opercularis to the subcentral region, including the inferior pre- and post-central gyri (Fig. 1, cluster 5). The temporal cortex includes the superior temporal, posterolateral temporal cortex extending to temporal and parietal junction, and anteromedial temporal cortex (Fig. 1, clusters 6 to 8). The parietal

[1]Department of Psychiatry, University of California, San Diego, La Jolla, CA 92093, USA. [2]Department of Cognitive Science, University of California, San Diego, La Jolla, CA 92093, USA. [3]Veterans Administration (VA) San Diego Healthcare System, San Diego, CA 92161, USA. [4]Department of Radiology, University of California, San Diego, La Jolla, CA 92093, USA. [5]VA Center of Excellence for Stress and Mental Health, San Diego, CA 92093, USA. [6]Departments of Psychiatry and Human and Molecular Genetics, Virginia Commonwealth University, Richmond, VA 23219, USA. [7]Center for Behavioral Genomics, University of California, San Diego, La Jolla, CA 92093, USA. [8]Department of Psychology, Boston University, Boston, MA 02215, USA. [9]Department of Radiology, Harvard Medical School and Massachusetts General Hospital, Boston, MA 02115, USA. [10]Department of Psychiatry, Harvard Medical School, Boston, MA 02215, USA. [11]Department of Neurosciences, University of California, San Diego, La Jolla, CA 92093, USA.

*These authors contributed equally to this work.
†To whom correspondence should be addressed. E-mail: wkremen@ucsd.edu